PRECLINICAL STUDIES

Ibrutinib as a potential therapeutic option for HER2 overexpressing breast cancer – the role of STAT3 and p21

Chandra Bose Prabaharan[1] · Allan Boyao Yang[2] · Divya Chidambaram[1] · Karthic Rajamanickam[1] · Scott Napper[3,4] · Meena Kishore Sakharkar[1]

Summary

Treatment response rates to current anticancer therapies for HER2 overexpressing breast cancer are limited and are associated with severe adverse drug reactions. Tyrosine kinases perform crucial roles in cellular processes by mediating cell signalling cascades. Ibrutinib is a recently approved Tyrosine Kinase Inhibitor (TKI) that has been shown be an effective therapeutic option for HER2 overexpressing breast cancer. The molecular mechanisms, pathways, or genes that are modulated by ibrutinib and the mechanism of action of ibrutinib in HER2 overexpressing breast cancer remain obscure. In this study, we have performed a kinome array analysis of ibrutinib treatment in two HER2 overexpressing breast cancer cell lines. Our analysis shows that ibrutinib induces changes in nuclear morphology and causes apoptosis via caspase-dependent extrinsic apoptosis pathway with the activation of caspases-8, caspase-3, and cleavage of PARP1. We further show that phosphorylated STAT3^{Y705} is upregulated and phosphorylated p21^{T145} is downregulated upon ibrutinib treatment. We propose that STAT3 upregulation is a passive response as a result of induction of DNA damage and downregulation of phosphorylated p21 is promoting cell cycle arrest and apoptosis in the two HER2 overexpressing cell lines. These results suggest that inhibitors of STAT3 phosphorylation may be potential options for combination therapy to help increase the efficacy of ibrutinib against HER2-overexpressing tumors.

Keywords Ibrutinib · BTK · Her2 + · STAT3 · p21

✉ Meena Kishore Sakharkar
meena.sakharkar@usask.ca

1 College of Pharmacy and Nutrition, University of Saskatchewan, 107 Wiggins Road, Saskatoon, SK S7N 5E5, Canada

2 Department of Anatomy, Physiology and Pharmacology, College of Medicine, University of Saskatchewan, 107 Wiggins Road, Saskatoon, SK S7N 5E5, Canada

3 Vaccine and Infectious Disease Organization-International Vaccine Research Centre, University of Saskatchewan, 120 Veterinary Road, Saskatoon, SK S7N 5E3, Canada

4 Department of Biochemistry, University of Saskatchewan, 107 Wiggins Road, Saskatoon, SK S7N 5E5, Canada

Introduction

In Canada, breast cancer affects 1 in 8 women and contributes to 13% of all cancer-related deaths in women (http://www.cancer.ca/en/cancer-information/cancer-type/breast/statistics/?region=on). In 2017, approximately 5,000 women died from breast cancer, and for many, metastatic breast cancer (MBC) is a significant contributing factor (diagnosed in nearly 30% of breast cancer patients) to patient mortality (90% of deaths) [1].

MBC is essentially incurable and existing treatments cause adverse events/side-effects [2, 3]. 25–30% of MBC patients overexpress epidermal growth factor receptor 2 (HER2) and this is associated with aggressive disease and poor prognosis [4].

Current targeted therapies for HER2-amplified breast cancer include trastuzumab, pertuzumab, and lapatinib. Trastuzumab (Herceptin) is a humanised IgG$_1$ antibody approved for the treatment of breast cancer (BC) cases that

overexpress HER2. A combination of trastuzumab with taxanes or anthracyclins shows improved efficacy and survival benefits [5, 6]. However, about 20–50% of patients initially selected for trastuzumab therapy do not respond to treatment and 70% of initial responders acquire resistance to trastuzumab (refractory disease) [7, 8]. Pertuzumab is a HER2 antibody that inhibits HER3 signalling by blocking ligand induced HER2-HER3 heterodimerization [9]. However, as with most antibodies their therapeutic benefits in preclinical and clinical studies have been modest and resistance is widespread [10].

Multi-target therapies, which modulate multiple key processes of cancer cell proliferation, migration, metabolism, anti-apoptotic signalling and drug resistance, have been shown to be effective in treating MBC [11]. A notable class of cancer targets are tyrosine kinases [12, 13], which mediate important cell signalling cascades. The tyrosine kinase inhibitors (TKIs) inhibit the aberrant tyrosine kinase signalling pathways in cancer (including breast cancer) [14]. Although marketed as inhibitors of a specific tyrosine kinase, TKIs normally have multiple kinase targets with different inhibitory potency [15]. Several TKIs like Neratinib, Sunitinib, Axitinib and Pazopinib have been implicated in the treatment of HER2 overexpressing BC either alone or in combination with Trastuzumab, other TKIs or chemotherapeutic agents, and each has its own limitations and advantages as they differentially target overlapping and non-overlapping cytoplasmic signalling pathways and proteins therein [16]. Hence, there is a continuing need to expand the array of TKIs as treatment options for HER2 overexpressing BC.

Ibrutinib is a recently approved TKI marketed as an irreversible inhibitor of Bruton's tyrosine kinase (BTK) for the treatment of B cell malignancies [17]. BTK functions as an important regulator of cell proliferation and cell survival and is pivotal in B cell receptor (BCR) signalling and other important signalling pathways [18]. A novel isoform of BTK has been shown to be over expressed in breast cancer cells and protect them from apoptosis [19]. Hendriks et al. highlighted the importance of BTK in various signalling pathways in the context of its therapeutic inhibition [18]. In a recent report, ibrutinib was shown to efficiently reduce the phosphorylation of HER1, HER2 and HER3 receptor tyrosine kinases in vitro underscoring the possibility of ibrutinib usage in HER2 overexpressing breast cancer therapeutics [20]. Ibrutinib in combination with Anti-PD-L1 (Anti-Programmed Death –L1) antibodies has been reported to have therapeutic effect in solid tumor animal models (mice) of triple negative breast cancer [21]. Recently, Chen et al. reported that ibrutinib functions as an irreversible inhibitor of HER2 and suggested that ibrutinib might enhance its own direct activity against HER2/EGFR via modulation of ITK and/or BTK [22]. Interestingly, it was recently shown that the effects of ibrutinib on HER2-positive breast cancer cells were not mitigated by NRG1

or EGF stimulation (as in the case of lapatinib) [23]. Also, the phosphorylation of HER2, BTK, AKT, and ERK and histone H3 was reduced by ibrutinib and cleaved caspase-3 signals were increased in breast cancer cells on treatment with ibrutinib [23].

Apart from the isolated reports on the effects of ibrutinib on HER2 overexpressing breast cancer and the role of ibrutinib in modulating EGFR signalling pathways, none of the studies on breast cancer demonstrate the molecular mechanisms, pathways, or genes that are modulated by ibrutinib and the mechanism of action of ibrutinib in HER2 overexpressing breast cancer remains obscure.

Phosphorylation is the predominant mechanism of post-translational modification for the regulation of protein function. With central roles in virtually every cellular process, and strong linkages with many diseases, there is a considerable interest in defining global cellular kinase activity (kinome). Within kinome analysis, peptide arrays have demonstrated considerable potential as a cost-effective, high-throughput approach for defining phosphorylation- mediated signal transduction activity.

Here, we use a novel and extensive peptide kinome array to study the effect of ibrutinib on two HER2 overexpressing breast cancer cells lines. This array provides information on cancer-associated pathways, proteins and phosphorylation events and queries 1290 phosphorylation events in major cancer signalling pathways. The peptides showing significant changes in the level of phosphorylation were further analysed computationally for gathering information on gene ontology and pathways. Selected proteins of interest were validated by western blot. The data on our investigations is presented.

Materials and methods

Antibodies and reagents

Monoclonal Antibodies against p-STAT3^{Y705}, p-p21^{T145}, caspase 8, casaspe3 and PARP1 were purchased from Abcam Inc., MA, USA. Antibodies against GAPDH and AKT were purchased from Cell Signaling Technologies, MA, USA. BTK siRNA and transfection reagents were purchased from Santa Cruz Biotechnology Inc., CA, USA. 4,5-dimethylthiazol-2-yl-2,5-diphenyltetrazolium bromide (MTT), Annexin V-FITC kit were purchased from Sigma Aldrich, USA. VECTASHIELD® Antifade Mounting Medium with DAPI was purchased from Vector Labs, USA. Ibrutinib (PCI-32765) was purchased from Selleckchem, TX, USA. Roswell Park Memorial Institute (RPMI) 1640 medium with L -glutamine, McCoy 5A medium, Phosphate Buffered Saline (1X PBS), and 0.25% Trypsin were purchased from HyClone, UT, USA. Fetal Bovine Serum (FBS) was obtained from Gibco Laboratories, MD, USA.

Cell lines and culture conditions

Cell lines were obtained from American Type Culture Collection (ATCC MD, USA). Human BT474 breast carcinoma cells were maintained in RPMI medium containing 10% Fetal Bovine Serum (FBS) and 2 mM L-glutamine at 37 °C and 5% CO_2. SKBR3 cells were maintained in RPMI medium containing 10% Fetal Bovine Serum (FBS) and 2 mM L-glutamine at 37 °C and 5% CO_2. Cultures were replenished with fresh medium every 2 to 3 days and passage 1:3 when they reached 80% confluence. The cells were regularly checked for *Mycoplasma* contamination.

MTT cell viability assay

The anti-proliferative effect of ibrutinib was assessed by MTT assay. MTT is a yellow colored tetrazole that is reduced to purple formazan in living cells. 5×10^3 cells per well (BT474 and SKBR3) were seeded in 96 well plates and incubated for 24 h individually. After incubation, the cells were treated with the desired concentration of Ibrutinib dissolved in Dimethyl sulfoxide (DMSO) for 72 h. Cells treated with DMSO were used as vehicle control and the growth medium was used as background (Blank) control. After treatment the cells were incubated with 100 μl of medium containing 4,5-dimethylthiazol-2-yl-2,5-diphenyltetrazolium bromide (MTT) with 5 mg/ml concentration at 37 °C for 4 h. This was followed by addition of 100 μl of DMSO to dissolve the formazan crystals, and the plates were read in synergy BioTek HT microplate reader at 570 nm. The experiment was performed in triplicate and mean value ± SD was calculated for each concentration. Cell viability was described as the ratio of absorbance (A_{570}nm) of treated cells versus the ratio of absorbance (A_{570}nm) of control cells [24, 25]. IC_{50} that is the concentration of ibrutinib needed to reduce 50% of absorbance relative to the vehicle (DMSO)-treated control was calculated using graph-pad Prism6 software.

Annexin V-propidium iodide analysis and flow cytometry analysis

The level of apoptosis in cancer cells on treatment with ibrutinib was assessed with Annexin V-propidium iodide kit. BT474 and SKBR3 cells were seeded (1×10^6 cell/well) in a 6 well plate (9 cm^2) individually to obtain 60–70% confluence in standard culture medium for 24 h. After treatment with Ibrutinib (IC50) for 72 h, the cells were trypsinized, washed, and incubated with Annexin V-FITC solution for 15 min (dark), as per manufacturer's instructions (APOAF - Annexin V-FITC Apoptosis Detection Kit, Sigma-Aldrich, St Louis, MO). After washing, the cells were analysed by flow cytometry immediately after propidium iodide solution was added (Cytoflex, Cytexpert, Beckman Coulter).

BTK knockdown using siRNA

The BTK gene expression in BT474 and SKBR3 cells was silenced (knock-down) using siRNA purchased from Santa Cruz Biotechnology Inc., CA, USA. The BTK siRNAs were transfected into cells according to the transfection protocol provided by Santa Cruz. The expression levels of BTK were determined using quantitative real time PCR. MTT assay (as described above) for cell viability was also performed, to check if silencing of BTK causes cell death and also to check if BTK inhibition is the only reason for cell death on treatment with ibrutinib.

Reverse transcription and quantitative real-time PCR

The expression level of BTK in the two HER2 overexpressing cell lines BT474 and SKBR3 was analysed by quantitative real time PCR (Applied biosystem Step one plus). Reverse transcription was performed using High capacity cDNA Reverse transcriptase kit (Applied Biosystem). The real time PCR reactions were performed using Bioline SensiFast SYBR green PCR Master Mix. forward primer sequence 5'-GGTGGAGAGCACGAGATAAA-3′ and reverse primer sequence 5'-CCGAGTCATGTGTTTGGAATAC-3′ were used to amplify BTK gene. GAPDH was used as the control [26]. The relative expression level of the gene of interest in different cDNA samples was determined using the $\Delta\Delta Ct$ method (http://www.gene-quantification.net/livak-2001.pdf). Ct value of the control (GAPDH) was subtracted from Ct value of the corresponding mRNA to get ΔCt value. Relative expression was measured by calculating $2-\Delta\Delta Ct$. Mean qRT – PCR threshold cycle (Ct) value is defined as the number of cycles required for the fluorescent signal to cross the threshold (i.e. 0.5 SD above background levels).

Nuclear morphology analysis / DAPI staining

BT474 and SKBR3 cells were seeded at a cell density of 2×10^5 cells on 35-mm cell culture plate and treated with IC_{50} of ibrutinib for 72 h. Following treatment, cells were fixed with 4% paraformaldehyde for 20 min, washed with PBS and mounted in 20 μl of Vectashield mounting medium containing 4′,6- diamidino-2 phenylindole (DAPI) (Vector Labs) for 10 min and the nuclei were observed using ZOE™ Fluorescence Cell Imager (Bio-Rad). DAPI is a blue coloured fluorescent DNA stain that shows enhancement in fluorescence upon binding to AT region of DNA.

Kinome profiling

Array design This work utilizes a peptide array customized to prioritize cancer-associated pathways, proteins and phosphorylation events [27]. Briefly, the 1290 phosphorylation events

represented on the array were derived from databases of experimentally defined phosphorylation events as well as phosphorylation events predicted by the software program DAPPLE2 [28]. Peptide substrates were selected to represent phosphorylation events known to be differentially regulated in a variety of cancers [29–31] as well as inclusion of major signaling pathways involved in proliferation, metabolism, and apoptosis to enable a broader perspective on signaling patterns.

Design, construction, and application of the peptide arrays were based upon a previously reported protocol with the modification that cells were serum-starved by growing in 0.5% FBS for 24 h prior to collection for kinome analysis [32, 33]. All data processing and analysis was done using the Platform for Intelligent, Integrated Kinome Analysis (PIIKA) software [33], which is freely available for noncommercial use at http://saphire.usask.ca/saphire/piika.

For hierarchical clustering of kinome data, the distance metric used was (1 - Pearson correlation), while McQuitty linkage was used as the linkage method. Colors indicate the average (over nine intra-array replicates) normalized phosphorylation intensity of each peptide, with blue indicating increased phosphorylation and white indicating decreased phosphorylation. The intensity of the color corresponds to the degree of increase or decrease [34].

Data analysis

Differential phosphoprotein expression

Data processing was performed in a web-based platform PIIKA 2 package [33] that analyses the raw intensities with background correction and computes the respective P-values (Benjamin–Hochberg false discovery rate). Fold changes in protein expression that correspond to changes in phosphorylation relative to control were calculated and subsequently analysed for the Differential Expression in Phosphoproteins (DEP) in comparison to respective control samples. DEPs with P-values <0.05 were considered significantly differentially expressed or modified relative to a control condition (DEP).

Heat map clustering for DEPs was performed using Heatmap.2 function in R/Bioconductor package "gplots" (http://cran.fhcrc.org/web/packages/gplots/gplots.pdf).

Functional gene annotation (gene ontology)

The differentially expressed proteins were submitted to the FunRich open access standalone enrichment analysis tool [35]. The FunRich standalone tool and GeneAlaCart package from Gene cards were used to derive information on gene ontology and super families based on gene names (provided in PIIKA array). FunRich analysis were performed to derive information on the biological processes, molecular functions and cellular location of these DEPs. GO terms with P value ≤0.05 were selected as significantly enriched and plotted.

Pathway over-representation analysis and pathway mapping

Pathway over-representation analysis was performed with InnateDB, a publicly available resource which, based on levels of either differential expression or phosphorylation, predicts biological pathways based on experiment fold change data sets [36]. Pathways were assigned a probability value (P) based on the number of proteins present for a particular pathway and the degree to which they were differentially expressed or modified relative to a control condition.

The proteins in the significantly modulated pathways were mapped on to the pathways using Pathview tool (KEGG pathway database platform) for the identification of the location of the protein the pathway [37] (data not shown).

Western blot analysis

After treatment of Ibrutinib, cells were trypsinized and washed with PBS for protein isolation. Whole cell lysates were prepared in lysis buffer (RIPA) containing 50 mM Tris (pH 8.0), 150 mM NaCl, 0.5 mM EDTA (pH 8.0), 1% Triton X-100, 0.5% Sodium deoxycholate and 0.1% SDS) enhanced with complete™ ULTRA Tablets of Protease inhibitor (Roche Applied Science) and phosphatase inhibitor (PhosStop, Roche Applied Science). Cell lysates were centrifuged at 14,000 rpm for 20 min at 4 °C and the supernatant was used for analyses of protein expression. Protein quantification was performed by Pierce™ BCA Protein Assay Kit (ThermoScientific, IL, USA). 25 μg of protein was loaded into SDS-polyacrylamide gels (10%) and electrophoresed at 100 V for 1.5 h. Following this, the proteins were transferred onto PVDF membranes (GE Healthcare, USA) for overnight and were then blocked using 5% non-fat milk (w/v) in TBS-0.1% Tween-20 at room temperature for 1 h. Membranes were incubated overnight at 4 °C with primary antibodies for anti p-STAT3^{Y705} (1:2000; Abcam), anti p-p21^{T145} (1:1000, Abcam), anti-AKT (1:1000; Cell Signaling Technologies), anti-Caspase 8 (1:1000; Abcam), anti-Caspase3 (1:1000; Abcam), anti-PARP1 (1:1000; Abcam) and anti-GAPDH (1:5000; Cell Signaling Technologies), respectively. GAPDH was used as a loading control. After probing, HRP conjugated secondary antibody was added and the membranes were incubated at room temperature for 1 h. Protein bands were developed using Clarity™ Western ECL blotting substrates and visualized using BIORAD Imager.
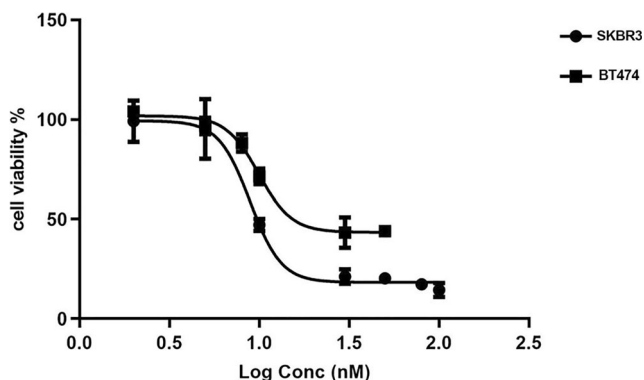
Results

Ibrutinib inhibits cell growth in breast cancer cell lines expressing HER2+ receptor

BT474 and SKBR3 cells were exposed to ibrutinib concentrations of 2, 5, 10, 30, and 50 nM for 24, 48 and 72 h, respectively. The cytotoxic and antiproliferative effect of ibrutinib was assessed by MTT dye reduction assay. The IC_{50} value for BT474 and SKBR3 were found to be 9.94 nM and 8.89 nM, respectively. We preferred to proceed with the respective IC_{50} concentrations to see the effects of Ibrutinib on both the cell lines. As shown in Fig. 1 cell numbers decreases in a dose-dependent fashion.

Ibrutinib inhibits cell proliferation by apoptosis

To elucidate whether the cytotoxic mode of action of ibrutinib is apoptosis or necrosis, flow cytometry analysis was performed on both BT474 and SKBR3 cells (treated at respective IC_{50} concentrations of 9.94 nM and 8.89 nM) using annexin V-FITC/PI. Simultaneous staining with annexin V-FITC and PI non-vital dye helps distinguish between intact cells (stained negative for both annexin V-FITC and PI), early apoptosis (stained positive for annexin V-FITC and negative for PI), and late apoptosis or cell death (stained positive for both and annexin V-FITC and PI).

In untreated BT474 culture, 78.04% of the cells were viable, 7.51% were in early apoptosis, and 11.33% were in the late or final stages of apoptosis. However, in ibrutinib-treated BT474 cells (72 h), 43.09% of the cells were viable, 37.76% were in early apoptosis and 17.61% were in the late or final stages of apoptosis. In SKBR3 untreated culture, 58.50% of the cells were viable, 20.06% were in early apoptosis, and 15.67% were in the late or final stages of apoptosis. However, in ibrutinib-treated SKBR3 cells (72 h), 32.23% of the cells were viable, 40.74% were in early apoptosis and

Fig. 1 IC_{50} values of Ibrutinib in two breast cancer cell lines overexpressing HER2 – BT474 and SKBR3. Cell viability was measure at exposure time of 72 h

23.92% were in the late or final stages of apoptosis (Fig. 2). These results suggest that ibrutinib inhibits cell proliferation in both the cell lines by apoptosis.

BTK is not the only target for ibrutinib

We performed quantitative RT-PCR and confirmed that stable knockdown of BTK is established in both BT474 and SKBR3 cells.. Quantitative RT-PCR data show that there is reduction in expression of BTK on treatment with siRNA for BTK. Interestingly, when the cells are treated with ibrutinib, a reduction in the expression of BTK was observed. This suggests that ibrutinib, an FDA approved BTK inhibitor, may also affect the transcription of gene *BTK* via a yet to be identified mechanism. However, when the cells were treated with ibrutinib and siRNA together, we do not observe a significant reduction in the expression of BTK (compared to individual treatments with siRNA and ibrutinib) in BT474. The difference in expression of BTK on treatment with a combination of ibrutinib and siRNA and siRNA and ibrutinib individually was significant for SKBR3. (Fig. 3a). One possibility could be that ibrutinib modulates a protein (kinase/non-kinase) that is directly or indirectly involved in regulating transcription of *BTK* in SKBR3 cells. Parallel investigations on cell viability using MTT assay show that treatment with siRNA for BTK alone does not cause a significant reduction in cell viability suggesting that BTK is not a key gene for cell survival in these two cell lines. Treatment with ibrutinib causes a significant reduction in cell viability in both cell lines. This can be explained based on the fact that ibrutinib being a tyrosine kinase inhibitor has multiple targets. Hence, inhibition of multiple targets concurrently is likely leading to cell death in both the cell lines. When the cells were treated with a combination of siRNA and ibrutinib, not much change in cell viability is observed in comparison to ibrutinib alone. This suggests that the function is dominated by ibrutinib in the treatment of breast cancer cells with a combination of ibrutinib and siRNA for BTK. In concordance, the expression data from The Cancer Genome Atlas (TCGA) shows that *BTK* is a not a key gene, whose expression is low and almost unaltered in Her2 overexpressing breast cancer. However, BTK is a key gene in lymphoma and leukemia and hence ibrutinib is marketed as a BTK inhibitor and a treatment option for B cell cancer. Since, ibrutinib has multiple targets, we propose that BTK is not the key target of ibrutinib in Her2 overexpressing breast cancer cell lines. (Fig. 3b).

Ibrutinib causes changes in nuclear morphology

In order to determine whether ibrutinib induces cell death by apoptosis, BT474 and SKBR3 cells were treated at IC_{50} concentrations of 9.94 nM and 8.89 nM at various time points such as 6, 12, 24, 48 and 72 h respectively. DAPI staining was
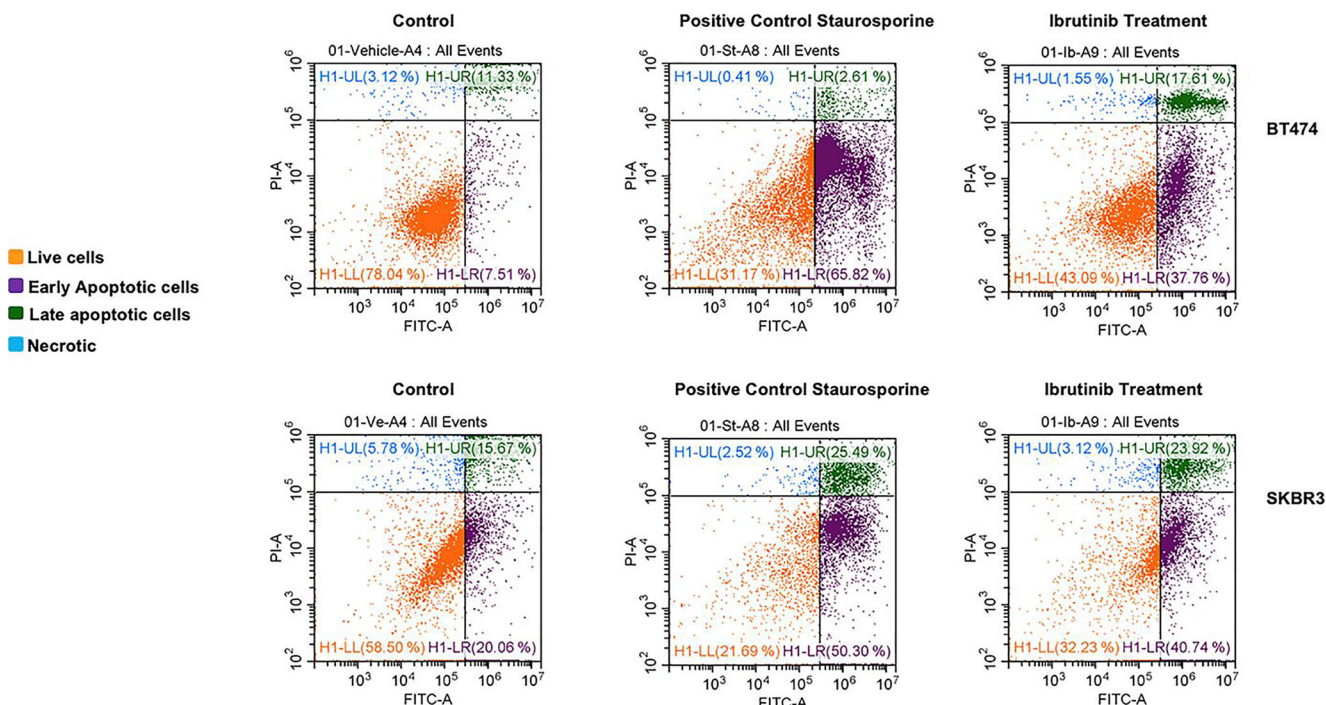
Fig. 2 Flow cytometry study of the effects of Ibrutinib on cell apoptosis and necrosis in BT474 and SKBR3 cells at exposure time of 72 h

performed to analyze the nuclear morphology for both the cell lines. Contrary to the control cells, we observed changes in nuclear morphology on treatment with ibrutinib at 48 and 72 h. Cell shrinkage, several condensed and fragmented nuclei representing alteration in nuclear morphology were observed in the ibrutinib treated cells in comparison to untreated control cells. (Fig. 4). This is characteristic of apoptosis. These results are in agreement with our Flow cytometry analyses.

Kinome Array - differential phosphoprotein expression

Kinome array shows that 404 proteins show significant change in phosphorylation in BT474 and 281 proteins show

significant change in phosphorylation in SKBR3 at a P value ≤0.05. The BT474 and SKBR3 share 209 DEPs. Interestingly, BT474 has 195 unique DEPs and SKBR3 has 72 DEPs. The volcano plots and Heatmap (Hierarchical clustering) are shown in Fig. 5. The proteins showing fold changes (FC) of ≤ −1.00 and ≥ 1.0 in phosphorylation when compared to the control are plotted against their corresponding P values using volcano plot (Fig. 5a) which is a scatterplot with FC on the x-axis and P value on the y-axis. The P value corresponds to the statistically significant difference between the phosphorylation level in the treatment and the phosphorylation level in the control and the fold-change (FC) value corresponds to the magnitude of the difference between the phosphorylation level in the treatment compared to the control (Fig. 5a).
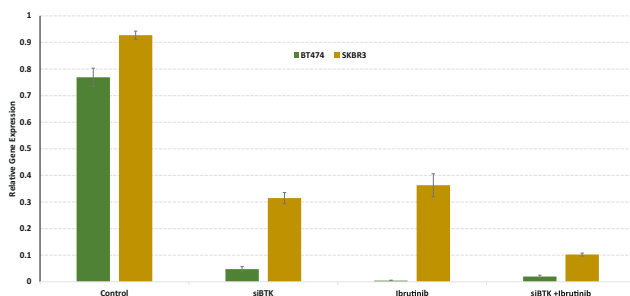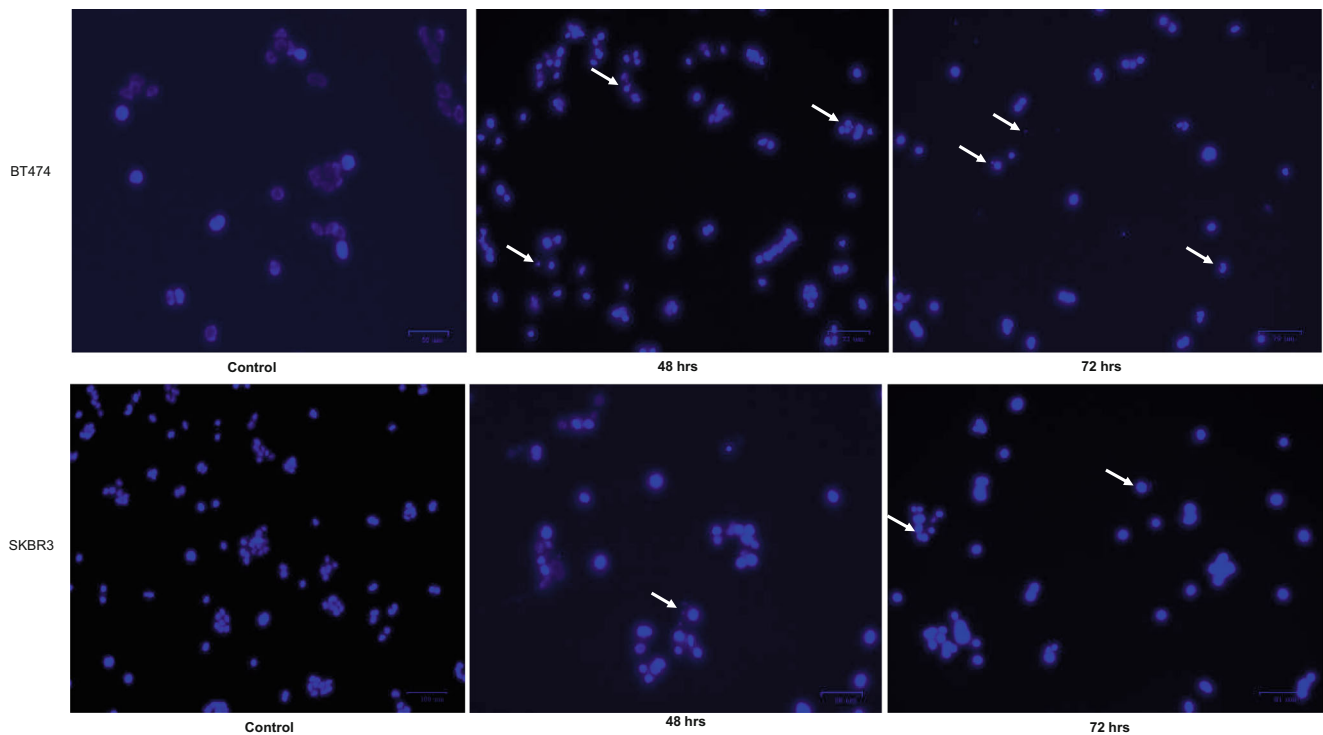

Fig. 3 a RT-PCR analysis of BTK knockdown efficiency in BT474 and SKBR3 cell lines, respectively. Data represent the means ±S.D. of three independent experiments. **$P < 0.01$, ***$P < 0.001$, compared with
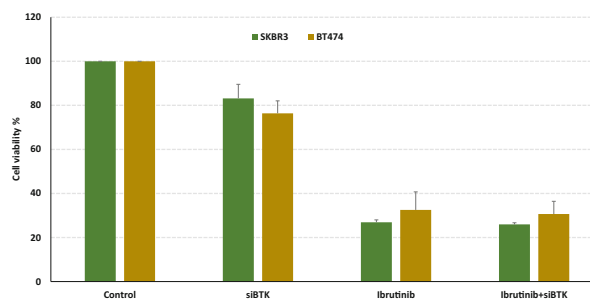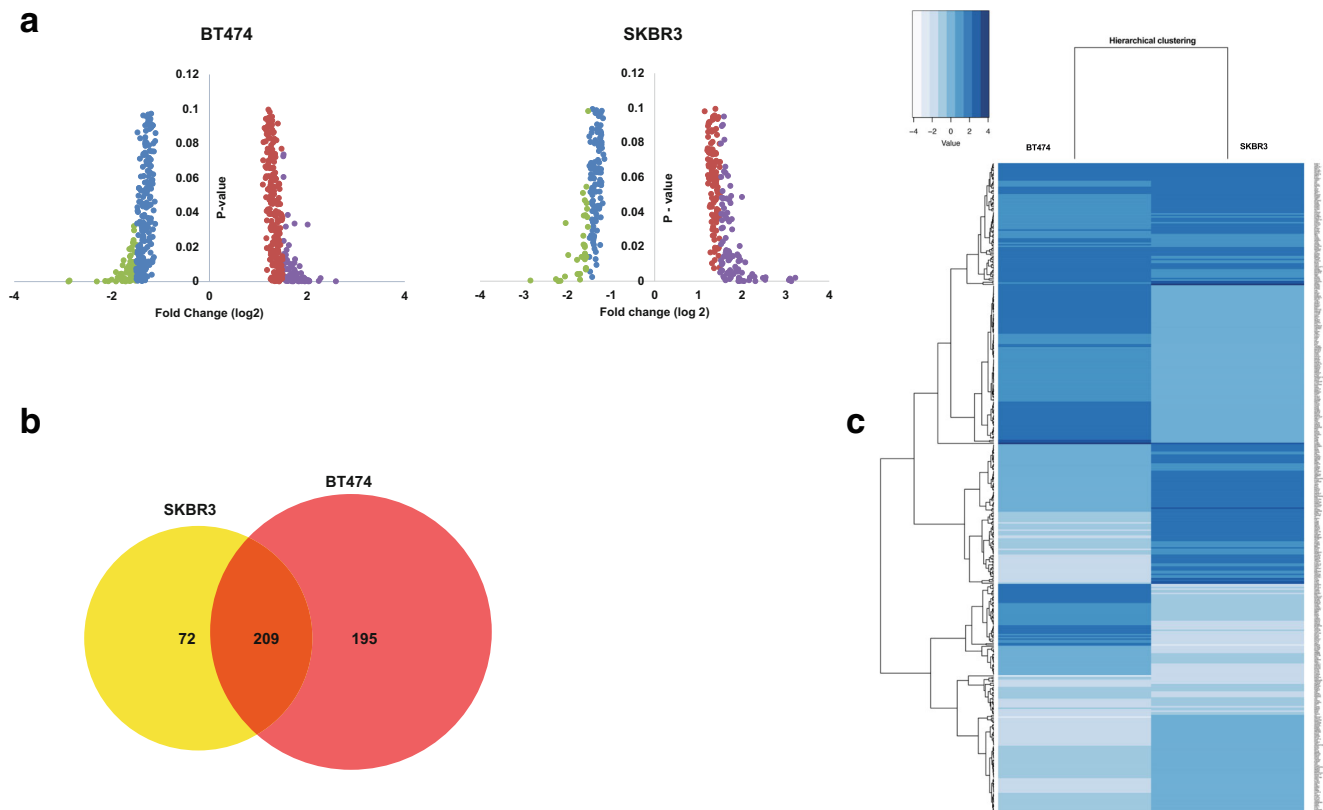
siRNA control. b MTT Assay showing cell viability after BTK knockdown and/or Ibrutinib treatment

Fig. 4 Ibrutinib treatment induces DNA fragmentation and apoptosis. DAPI-stained micrographs for control, 48 h and 72 h drug exposure in BT474 and SKBR3 cells using a ZOE fluorescent cell imager. Arrows indicate condensed and fragmented nuclei

Fig. 5 **a** Volcano plots showing the distribution of the fold changes in DEPs. Phosphoproteins with fold change ≥1.00 and ≤1.5 are shown in red, ≥1.5 as purple, ≥−1.00 and ≤−1.5 as blue and ≤−1.5 as green. **b** The

Venn diagram represent the DEPs that are common and unique in the two cell lines. **c** Heat map representing hierarchical clustering Of the DEPs in the two cell lines

The proteins showing fold changes (FC) of ≤ −1.00 and ≥ 1.0 and shared and unique across the two breast cancer cell lines under investigation are also represented using a Venn diagram (Fig. 5b).

Heat map allows for visualisation in the difference between the phosphorylation level in the treatment compared to the control and across the two cell lines using a color code gradient. (Fig. 5c).

Gene ontology and pathway analyses

We analyzed the GO terms for all the DEPs in both the cell lines BT474 and SKBR3 using FunRich (Supplementary – Figure - S1a and S1b). The analysis revealed that protein phosphorylation (79), signal transduction (66), and positive regulation of transcription from RNA polymerase II promoter (57) are the most common GO categories ($P \leq 0.05$) represented in biological processes; ATP binding (139), protein kinase binding (50), and metal ion binding (47) are the most common GO categories in molecular function and cytoplasm (160), plasma membrane (159), and nucleus (158) are the most common categories in cellular location in BT474. The analysis revealed that protein phosphorylation (50), signal transduction(47), and negative regulation of apoptotic process (38) are the most common GO categories ($P \leq 0.05$) represented in biological processes; protein binding (218), protein kinase activity (32), and metal ion binding (30) are the most common GO categories in Molecular function and plasma membrane (123), cytoplasm (122), and nucleus (118) are the most common categories in cellular location in SKBR3.

Pathway enrichment

The proteins showing fold changes (FC) of ≤ −1.00 and ≥ 1.0 in BT474 and SKBR3 were classified into superfamilies. This allows for categorising the proteins into different biological pathways. The top 10 significant biological pathways for both BT474 and SKBR3 are shown in Supplementary – Figure S2a and S2b. The top four most represented biological pathways are EPO signaling pathway, IL-7 signaling pathway, VEGF signaling pathway and JAK-STAT. Since, JAK-STAT pathway was of our interest, the genes in the JAK-STAT pathway are shown in a Circos plot (R Package). Circos plot illustrates the genes in the chosen pathway and their associated GO terms. (Fig. 6).

## Effect of ibrutinib on STAT3-p21 axis and the apoptotic pathway

The JAK-STAT pathway has 76 and 54 proteins that show changes in phosphorylation levels on treatment with ibrutinib in BT474 and SKBR3 cell lines, respectively. p-STAT3^{Y705} is an important protein involved in transcription and isolated reports suggest on its apoptotic activity. Since we observed apoptotic cell death (flow cytometry) and changes in nuclear morphology (DAPI), we estimated the changes in the expression of p-STAT3^{Y705} and p-p21^{T145} and the proteins bringing about apoptosis (Caspase 3, 8 and PARP1) (Fig. 7). There was increase in the expression of p-STAT3^{Y705} and decrease in the expression level of p- p21^{T145} in a time dependent manner. This is consistent with previous reports [22]. It was observed that the level of expression of pro-caspase-8, pro-caspase-3, and PARP1 are decreased on treatment with ibrutinib. (Fig. 7).

Discussion

Treatment response rates to current anticancer therapies for HER2 overexpressing breast cancer (BC) are disappointingly low and have undesirable side effects [38]. Hence, there is a need to find new treatment options for HER2 overexpressing breast cancer. Tyrosine kinases mediate cell signalling cascades and perform crucial roles in cellular processes like growth, differentiation, metabolism and apoptosis, and hence TKIs (Tyrosine Kinase Inhibitors) impose important therapeutic effects in complex diseases like HER2 overexpressing BC. Ibrutinib is a recently approved TKI for BTK. It covalently binds to the cysteine residue (Cys-481) near the ATP-binding pocket of BTK and irreversibly inhibits BTK [39]. Interestingly, statistically significant association of expression of BTK with HER2 expression has also been reported [23]. Recently, Chen et al. performed a high-throughput screening of ibrutinib for growth inhibitory activity against two panels of tumor cell lines, a 230-cancer cell panel and the NCI-60 panel and other breast cancer cell lines (MDA-MB-453, SKBR3, and UACC-893) [22]. It was reported that breast cancer lines with HER2 overexpression (except MDA-MB-361) were most significantly inhibited by ibrutinib (<100 nM) with the IC$_{50}$ lower than that of lapatinib and dacomitinib [22]. Although, the BTK inhibitor ibrutinib has been reported to be effective in HER2 overexpressing cell lines and studies suggest that it reduces the phosphorylation of the receptor tyrosine kinases HER1, HER2 and HER3 in HER2 overexpressing breast cancer cell lines, its exact mode of action is not known. Sequence alignment results have been reported to show that 10 kinases in the human genome could be potential targets of ibrutinib as they have a cysteine residue at an analogous position to the cysteine residue (Cys-481) near the ATP-binding pocket of BTK. These are Blk, Btk, Bmx, EGFR, HER2, ErbB4, Itk, Jak3, Tec, and Txk [23]. Ibrutinib has been shown to cause reduction of phosphorylation of HER2, BTK, AKT, ERK and histone H3 and increase in cleaved caspase-3 signals resulting in inhibition of growth in a HER2 overexpressing xenograft model [23]. Ibrutinib has also been reported to inhibit PLCγ1, PLCγ2, AKT, and ERK phosphorylation, and cause increase in cleavage of PARP1 in HER2 overexpressing BT474 cell line [23]. PARP1 is a
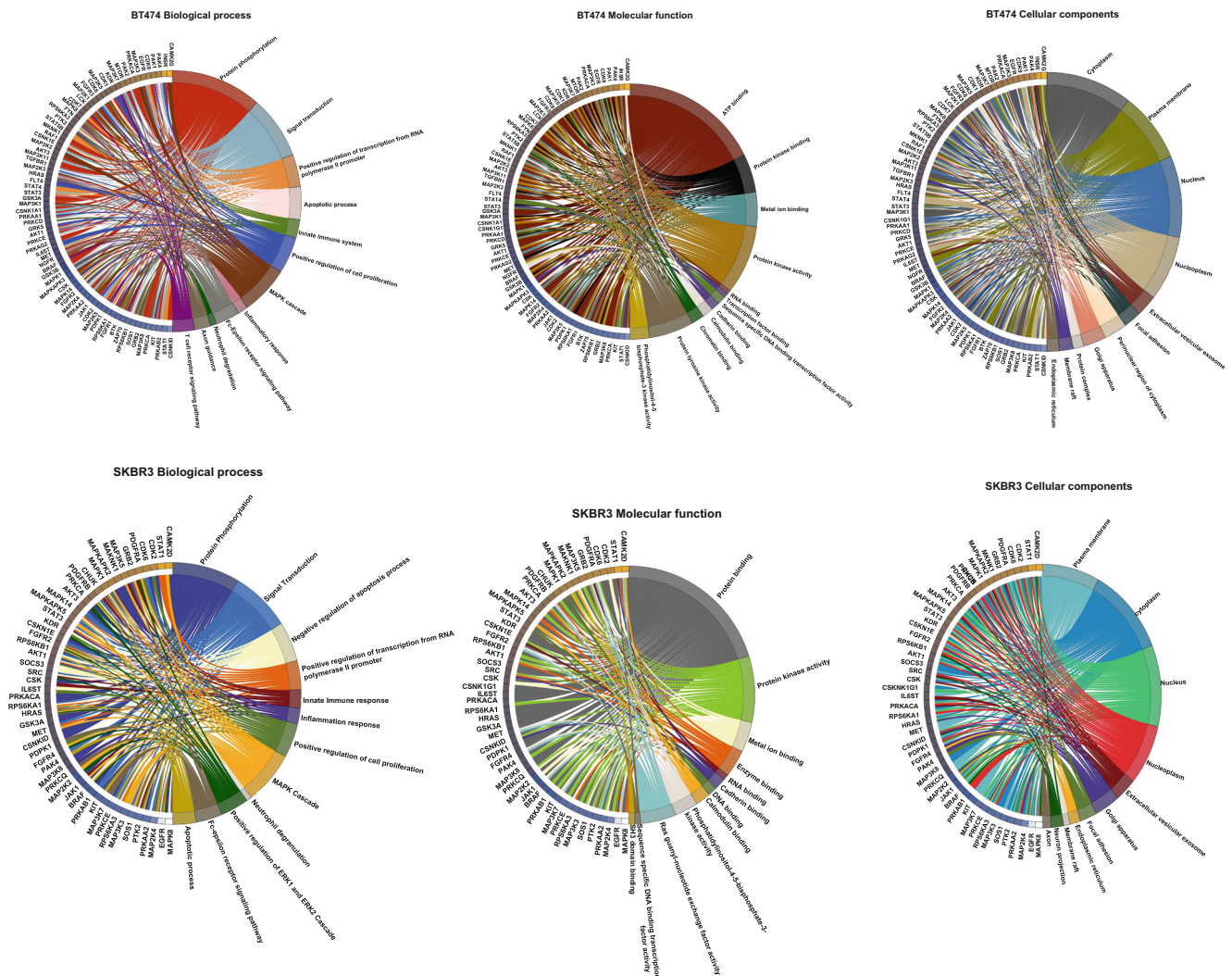
Fig. 6 Circos plot representing gene ontology terms enriched in the JAK-STAT pathway for biological process, molecular function and Cellular component and the associated genes. Gene names are arranged (clockwise) in order of their fold change starting from most down-regulated on treatment with ibrutinib in BT474 and SKBR3 cells

nuclear protein and is the key enzyme associated with the repair of damaged DNA [40]. Since our flow cytometry analysis showed apoptosis as a mechanism of cell death, we embarked on elucidating and analysing the mechanism of apoptosis. A diverse array of physiological and pathological stimuli and conditions can initiate apoptosis. DAPI staining of ibrutinib treated and control cells showed changes in nuclear morphology, which can be attributed to apoptosis as apoptosis can cause changes and morphological alterations of the cell nucleus. It has been reported that ibrutinib treatment causes an increase in caspase 3 cleavage, suggesting caspase medicated apoptosis. Here, we showed that ibrutinib induced apoptosis via caspase-dependent extrinsic apoptosis pathway showing changes in expression of pro-caspases-8, pro-caspase-3, and PARP1. Since (PARP) Poly (ADP-ribose) polymerase (PARP) family of proteins play important roles in cellular processes such as DNA repair, genomic stability, and

programmed cell death, the results suggest that ibrutinib has anticancer effects with respect to its ability to affect the DNA repair mechanism and activate the effector caspase through extrinsic pathway which may be one of the factors leading to apoptosis.

Superfamily distribution data for the DEP shows that proteins in EPO signalling superfamily, IL-7 immune system superfamily, VEGF signaling and JAK-STAT signalling superfamily are most highly represented in the ibrutinib kinome array in both the cell lines. Chen et al. have reported that ibrutinib inhibits cell growth by downregulating phosphorylation on HER2 and EGFR and their downstream targets, p-AKT and ERK [22]. Here, for the first time we report on the role of STAT3 pathway in the anti-proliferative activity of ibrutinib in breast cancer cell lines BT474 and SKBR3.

A complex array of activities and functions in tumorigenesis are modulated by STAT3. [41]. STAT3 activation is
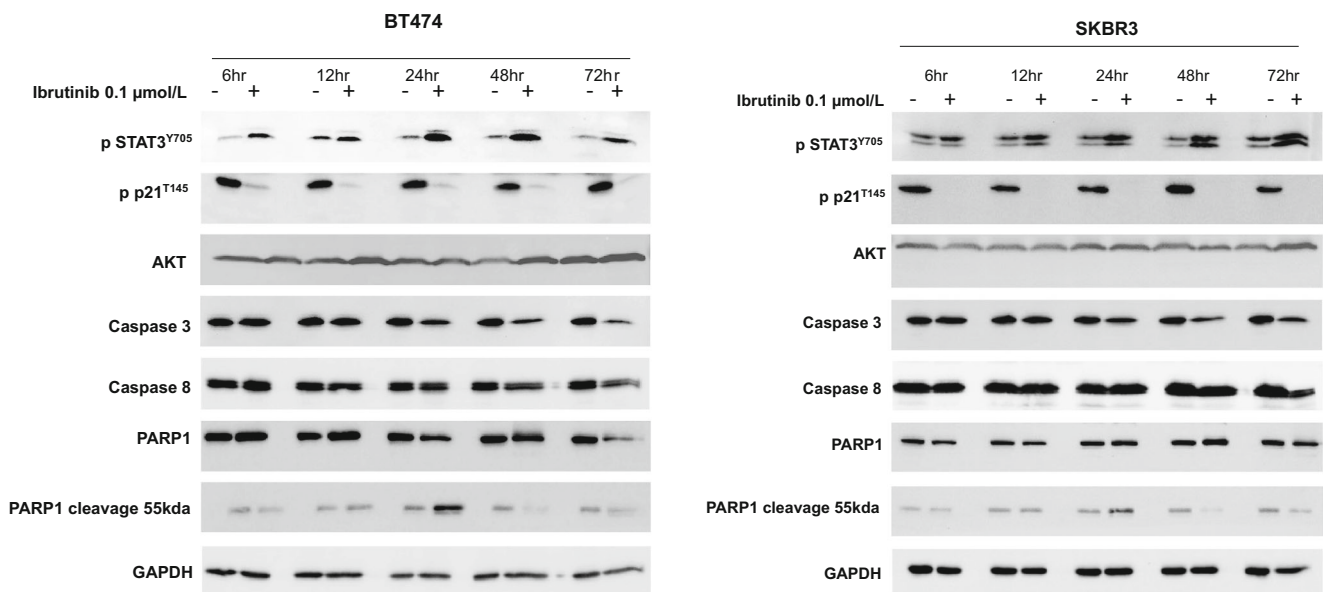
BT474

SKBR3

Fig. 7 Changes in expression of p-STAT3, p-p21, AKT, pro-caspase-3, pro-caspase-8, PARP1 proteins in BT474 and SKBR3 cells upon treatment with 0.1 μM Ibrutinib for 6 h, 12 h, 24 h, 48 h and 72 h. respectively. GAPDH is used as loading control

known to rely on the phosphorylation of a tyrosine residue (Y705) that induces its dimerization, nuclear translocation, and DNA binding [22]. Y705-phosphorylation of STAT3 was observed to be significantly upregulated upon ibrutinib treatment in our kinome array and western blot analyses.

Phosphorylated $STAT3^{Y705}$ has transcriptional activity and modulates the expression of several genes involved in cancer etiology, such as tumor immune surveillance, metastasis, tumor angiogenesis, and oncogenic cell signalling [42]. Although activated STAT3 is involved in biochemical
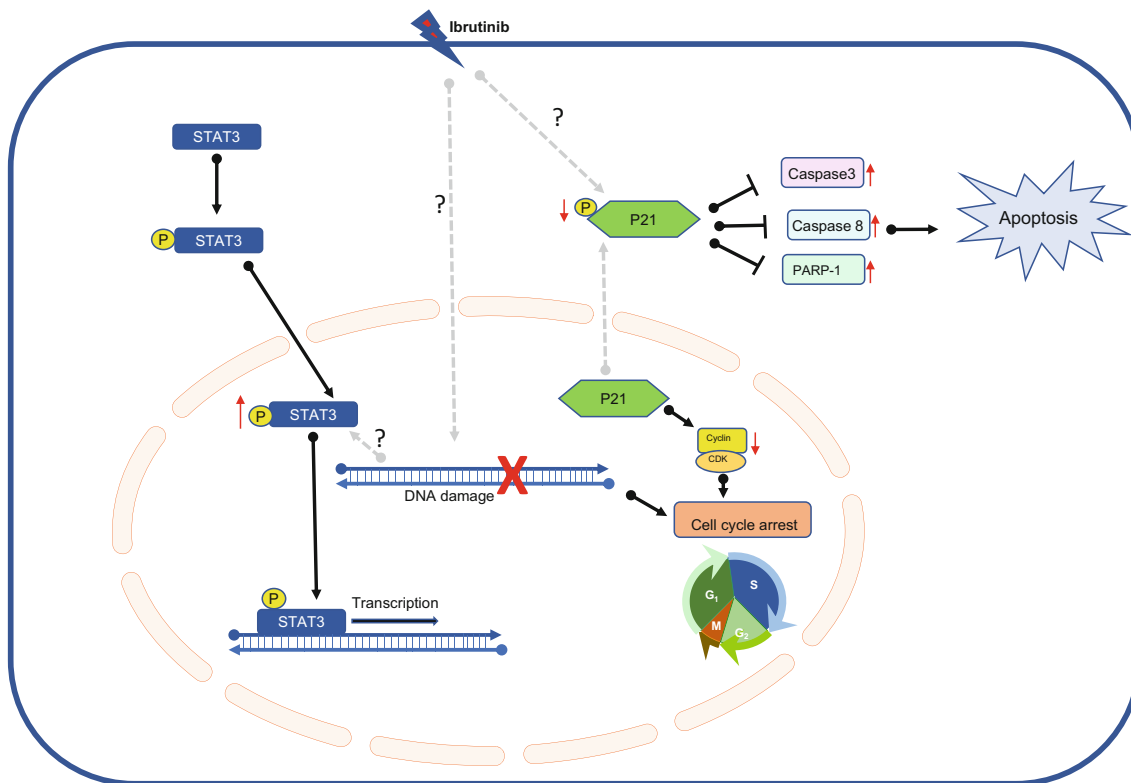
Fig. 8 Schematic representation showing proposed mechanism of action of Ibrutinib

aberrancy of cancer cells and contributes to tumorigenesis, several recent studies indicate that STAT3 may exert tumor suppressor effects under specific conditions [43–47]. It has been reported that tumor cells exposed to DNA damage increase the expression and secretion of IL-6 and the phosphorylation of JAK1 and STAT3. STAT3^{Y705} has been reported to inhibit growth recovery from DNA damage-induced arrest. This STAT3 phosphorylation and modulation of JAK1–STAT3 signalling pathway acts as a passive response and promotes growth recovery after DNA damage [48].

DNA damage has been reported to induce cell cycle arrest. Interestingly, Chen et al. have reported that ibrutinib treatment in HER2 overexpressing breast cancer cell lines causes growth inhibition by arresting the cells in G1 phase of cell cycle [22]. It is known that both G1 and G2 checkpoints are modulated by transcriptional targets of p53 [49] p21WAF1/CIP1 (hereafter referred to as p21) can be induced by both p53-dependent and p53-independent mechanisms and is also a universal inhibitor of cyclin-dependent kinases [50]. It is also one of the target genes activated by the JAK-STAT cascade. Our investigations show that T145-phosphorylation of p21 was downregulated upon ibrutinib treatment. Interestingly, p21 can function both as a tumor suppressor and an oncogene, depending primarily on its subcellular location [51]. The tumor-suppressive activities of p21 are associated with its nuclear localization, whereas cytoplasmic p21 contributes to its oncogenic effects. T145 phosphorylation can induce the relocalization of p21 from nucleus to cytosol [52]. Cytoplasmic localization of p21 after T145 phosphorylation has also been reported to be associated with anti-apoptotic activity of p21 [53]. Since our data shows decrease in phosphorylated p21 on treatment with ibrutinib, it is an indicator of apoptotic activity of p21. However, the exact mechanism needs further elucidation [54–57]. Nonetheless, the mechanisms by which p21 promotes apoptosis has been suggested to be related to its interaction with DNA repair machinery [58]. Thus, we propose (hypothesise) that STAT3 upregulation is a passive response as a result of an induction of DNA damage on treatment of ibrutinib and downregulation of phosphorylated p21 promotes cell cycle arrest and apoptosis in the two HER2 overexpressing cell lines under investigation (Fig. 8). As shown earlier, this apoptosis is mediated by caspase-3, caspase-8, and PARP1 cleavage. However, this hypothesised pathway needs to be validated by further experiments.

Interestingly, STAT3 phosphorylation inhibitors have been shown to exhibit potent growth suppressive activity in pancreatic and breast cancer cells [59]. Also relationship between, pSTAT3 and trastuzumab resistance in HER2-positive primary breast cancers has also been reported [60]. unphosphorylated form of STAT3 has been reported to bind to regulatory regions of proapoptotic genes and prevents their expression in prostate tumor cells but not normal cells [61]. These results suggest that inhibitors of STAT3 phosphorylation may be potential option as a promising strategies for combination therapy to help increase the efficacy of ibrutinib against HER2-overexpressing tumors.

Compliance with ethical standards

Conflict of interest All authors declare that they have no conflict of interest.

Ethical approval This article does not contain any studies with human participants or animals performed by any of the authors.

Informed consent For this type of study, formal consent is not required.

References

1. DeSantis C, Ma J, Bryan L, Jemal A (2014) Breast cancer statistics, 2013. CA Cancer J Clin 64(1):52–62. https://doi.org/10.3322/caac.21203

2. Irvin W Jr, Muss HB, Mayer DK (2011) Symptom management in metastatic breast cancer. Oncologist 16(9):1203–1214. https://doi.org/10.1634/theoncologist.2011-0159

3. Lluch A, Alvarez I, Munoz M, Segui MA, Tusquets I, Garcia-Estevez L (2014) Treatment innovations for metastatic breast cancer: nanoparticle albumin-bound (NAB) technology targeted to tumors. Crit Rev Oncol Hematol 89(1):62–72. https://doi.org/10.1016/j.critrevonc.2013.08.001

4. O'Sullivan CC, Smith KL (2014) Therapeutic considerations in treating HER2-positive metastatic breast Cancer. Curr Breast Cancer Rep 6(3):169–182. https://doi.org/10.1007/s12609-014-0155-y

5. Jahanzeb M (2008) Adjuvant trastuzumab therapy for HER2-positive breast cancer. Clin Breast Cancer 8(4):324–333. https://doi.org/10.3816/CBC.2008.n.037

6. Slamon DJ, Leyland-Jones B, Shak S, Fuchs H, Paton V, Bajamonde A, Fleming T, Eiermann W, Wolter J, Pegram M, Baselga J, Norton L (2001) Use of chemotherapy plus a monoclonal antibody against HER2 for metastatic breast cancer that overexpresses HER2. N Engl J Med 344(11):783–792. https://doi.org/10.1056/NEJM200103153441101

7. Harris LN, You F, Schnitt SJ, Witkiewicz A, Lu X, Sgroi D, Ryan PD, Come SE, Burstein HJ, Lesnikoski BA, Kamma M, Friedman PN, Gelman R, Iglehart JD, Winer EP (2007) Predictors of resistance to preoperative trastuzumab and vinorelbine for HER2-positive early breast cancer. Clin. Cancer Res 13(4):1198–1207. https://doi.org/10.1158/1078-0432.CCR-06-1304

8. Wolff AC, Hammond ME, Schwartz JN, Hagerty KL, Allred DC, Cote RJ, Dowsett M, Fitzgibbons PL, Hanna WM, Langer A, McShane LM, Paik S, Pegram MD, Perez EA, Press MF, Rhodes A, Sturgeon C, Taube SE, Tubbs R, Vance GH, van de Vijver M, Wheeler TM, Hayes DF, American Society of Clinical Oncology/College of American P (2007) American Society of Clinical Oncology/College of American Pathologists guideline recommendations for human epidermal growth factor receptor 2 testing in breast cancer. Arch Pathol Lab Med 131 (1):18–43. doi:https://doi.org/10.1043/1543-2165(2007)131[18:ASOCCO]2.0.CO;2

9. Lee-Hoeflich ST, Crocker L, Yao E, Pham T, Munroe X, Hoeflich KP, Sliwkowski MX, Stern HM (2008) A central role for HER3 in HER2-amplified breast cancer: implications for targeted therapy. Cancer Res 68(14):5878–5887. https://doi.org/10.1158/0008-5472.CAN-08-0380

10. Kruser TJ, Wheeler DL (2010) Mechanisms of resistance to HER family targeting antibodies. Exp Cell Res 316(7):1083–1100. https://doi.org/10.1016/j.yexcr.2010.01.009

11. Tang J, Aittokallio T (2014) Network pharmacology strategies toward multi-target anticancer therapies: from computational models to experimental design principles. Curr Pharm Des 20(1):23–36

12. Tang J, Karhinen L, Xu T, Szwajda A, Yadav B, Wennerberg K, Aittokallio T (2013) Target inhibition networks: predicting selective combinations of druggable targets to block cancer survival pathways. PLoS Comput Biol 9(9):e1003226. https://doi.org/10.1371/journal.pcbi.1003226

13. Zhang J, Yang PL, Gray NS (2009) Targeting cancer with small molecule kinase inhibitors. Nat Rev Cancer 9(1):28–39. https://doi.org/10.1038/nrc2559

14. Paul MK, Mukhopadhyay AK (2004) Tyrosine kinase - role and significance in Cancer. Int J Med Sci 1(2):101–115

15. Davis MI, Hunt JP, Herrgard S, Ciceri P, Wodicka LM, Pallares G, Hocker M, Treiber DK, Zarrinkar PP (2011) Comprehensive analysis of kinase inhibitor selectivity. Nat Biotechnol 29(11):1046–1051. https://doi.org/10.1038/nbt.1990

16. Mundhenke C, Strauss A, Schem C (2009) Significance of tyrosine kinase inhibitors in the treatment of metastatic breast Cancer. Breast Care (Basel) 4(6):373–378. https://doi.org/10.1159/000261705

17. Honigberg LA, Smith AM, Sirisawad M, Verner E, Loury D, Chang B, Li S, Pan Z, Thamm DH, Miller RA (2010) The Bruton tyrosine kinase inhibitor PCI-32765 blocks B-cell activation and is efficacious in models of autoimmune disease and B-cell malignancy. Proc Natl Acad Sci 107(29):13075–13080

18. Hendriks RW, Yuvaraj S, Kil LP (2014) Targeting Bruton's tyrosine kinase in B cell malignancies. Nat Rev Cancer 14(4):219–232. https://doi.org/10.1038/nrc3702

19. Eifert C, Wang X, Kokabee L, Kourtidis A, Jain R, Gerdes MJ, Conklin DS (2013) A novel isoform of the B cell tyrosine kinase BTK protects breast cancer cells from apoptosis. Genes Chromosom Cancer 52(10):961–975. https://doi.org/10.1002/gcc.22091

20. Grabinski N, Ewald F (2014) Ibrutinib (ImbruvicaTM) potently inhibits ErbB receptor phosphorylation and cell viability of ErbB2-positive breast cancer cells. Investig New Drugs 32(6):1096–1104. https://doi.org/10.1007/s10637-014-0141-2

21. Sagiv-Barfi I, Kohrt HE, Czerwinski DK, Ng PP, Chang BY, Levy R (2015) Therapeutic antitumor immunity by checkpoint blockade is enhanced by ibrutinib, an inhibitor of both BTK and ITK. Proc Natl Acad Sci U S A 112(9):E966–E972. https://doi.org/10.1073/pnas.1500712112

22. Chen J, Kinoshita T, Sukbuntherng J, Chang BY, Elias L (2016) Ibrutinib inhibits ERBB receptor tyrosine kinases and HER2-amplified breast Cancer cell growth. Mol Cancer Ther 15(12):2835–2844. https://doi.org/10.1158/1535-7163.MCT-15-0923

23. Wang X, Wong J, Sevinsky CJ, Kokabee L, Khan F, Sun Y, Conklin DS (2016) Bruton's tyrosine kinase inhibitors prevent therapeutic escape in breast Cancer cells. Mol Cancer Ther 15(9):2198–2208. https://doi.org/10.1158/1535-7163.MCT-15-0813

24. Looi CY, Arya A, Cheah FK, Muharram B, Leong KH, Mohamad K, Wong WF, Rai N, Mustafa MR (2013) Induction of apoptosis in human breast cancer cells via caspase pathway by vernodalin isolated from Centratherum anthelminticum (L.) seeds. PLoS One 8(2):e56643. https://doi.org/10.1371/journal.pone.0056643

25. Riss TL, Moravec RA, Niles AL, Duellman S, Benink HA, Worzella TJ, Minor L (2004) Cell viability assays. In: Sittampalam GS, Coussens NP, Brimacombe K et al. (eds) Assay Guidance Manual. Bethesda (MD),

26. Wang JD, Chen XY, Ji KW, Tao F (2016) Targeting Btk with ibrutinib inhibit gastric carcinoma cells growth. Am J Transl Res 8(7):3003–3012

27. Smith SE, Mellor P, Ward AK, Kendall S, McDonald M, Vizeacoumar FS, Vizeacoumar FJ, Napper S, Anderson DH (2017) Molecular characterization of breast cancer cell lines through multiple omic approaches. Breast Cancer Res 19(1):65. https://doi.org/10.1186/s13058-017-0855-0

28. Trost B, Arsenault R, Griebel P, Napper S, Kusalik A (2013) DAPPLE: a pipeline for the homology-based prediction of phosphorylation sites. Bioinformatics 29(13):1693–1695. https://doi.org/10.1093/bioinformatics/btt265

29. Baine MJ, Chakraborty S, Smith LM, Mallya K, Sasson AR, Brand RE, Batra SK (2011) Transcriptional profiling of peripheral blood mononuclear cells in pancreatic cancer patients identifies novel genes with potential diagnostic utility. PLoS One 6(2):e17014. https://doi.org/10.1371/journal.pone.0017014

30. Dhanasekaran SM, Barrette TR, Ghosh D, Shah R, Varambally S, Kurachi K, Pienta KJ, Rubin MA, Chinnaiyan AM (2001) Delineation of prognostic biomarkers in prostate cancer. Nature 412(6849):822–826. https://doi.org/10.1038/35090585

31. Twine NC, Stover JA, Marshall B, Dukart G, Hidalgo M, Stadler W, Logan T, Dutcher J, Hudes G, Dorner AJ, Slonim DK, Trepicchio WL, Burczynski ME (2003) Disease-associated expression profiles in peripheral blood mononuclear cells from patients with advanced renal cell carcinoma. Cancer Res 63(18):6069–6075

32. Jalal S, Arsenault R, Potter AA, Babiuk LA, Griebel PJ, Napper S (2009) Genome to kinome: species-specific peptide arrays for kinome analysis. Sci Signal 2(54):pl1. https://doi.org/10.1126/scisignal.254pl1

33. Trost B, Kindrachuk J, Maattanen P, Napper S, Kusalik A (2013) PIIKA 2: an expanded, web-based platform for analysis of kinome microarray data. PLoS One 8(11):e80837. https://doi.org/10.1371/journal.pone.0080837

34. Li Y, Arsenault RJ, Trost B, Slind J, Griebel PJ, Napper S, Kusalik A (2012) A systematic approach for analysis of peptide array kinome data. Sci Signal 5 (220):pl2. https://doi.org/10.1126/scisignal.2002429

35. Pathan M, Keerthikumar S, Ang CS, Gangoda L, Quek CY, Williamson NA, Mouradov D, Sieber OM, Simpson RJ, Salim A, Bacic A, Hill AF, Stroud DA, Ryan MT, Agbinya JI, Mariadason JM, Burgess AW, Mathivanan S (2015) FunRich: an open access standalone functional enrichment and interaction network analysis tool. Proteomics 15(15):2597–2601. https://doi.org/10.1002/pmic.201400515

36. Lynn DJ, Winsor GL, Chan C, Richard N, Laird MR, Barsky A, Gardy JL, Roche FM, Chan TH, Shah N, Lo R, Naseer M, Que J, Yau M, Acab M, Tulpan D, Whiteside MD, Chikatamarla A, Mah B, Munzner T, Hokamp K, Hancock RE, Brinkman FS (2008) InnateDB: facilitating systems-level analyses of the mammalian innate immune response. Mol Syst Biol 4:218. https://doi.org/10.1038/msb.2008.55

37. Luo W, Pant G, Bhavnasi YK, Blanchard SG Jr, Brouwer C (2017) Pathview web: user friendly pathway visualization and data integration. Nucleic Acids Res 45(W1):W501–W508. https://doi.org/10.1093/nar/gkx372

38. Larionov AA (2018) Current therapies for human epidermal growth factor receptor 2-positive metastatic breast Cancer patients. Front Oncol 8:89. https://doi.org/10.3389/fonc.2018.00089

39. Wang A, Yan XE, Wu H, Wang W, Hu C, Chen C, Zhao Z, Zhao P, Li X, Wang L, Wang B, Ye Z, Wang J, Wang C, Zhang W, Gray NS, Weisberg EL, Chen L, Liu J, Yun CH, Liu Q (2016) Ibrutinib targets mutant-EGFR kinase with a distinct binding conformation.

Oncotarget 7(43):69760–69769. https://doi.org/10.18632/oncotarget.11951

40. Ko HL, Ren EC (2012) Functional aspects of PARP1 in DNA repair and transcription. Biomolecules 2(4):524–548. https://doi.org/10.3390/biom2040524

41. Carpenter RL, Lo HW (2014) STAT3 target genes relevant to human cancers. Cancers (Basel) 6(2):897–925. https://doi.org/10.3390/cancers6020897

42. Timofeeva OA, Tarasova NI, Zhang X, Chasovskikh S, Cheema AK, Wang H, Brown ML, Dritschilo A (2013) STAT3 suppresses transcription of proapoptotic genes in cancer cells with the involvement of its N-terminal domain. Proc Natl Acad Sci U S A 110(4):1267–1272. https://doi.org/10.1073/pnas.1211805110

43. de la Iglesia N, Konopka G, Puram SV, Chan JA, Bachoo RM, You MJ, Levy DE, Depinho RA, Bonni A (2008) Identification of a PTEN-regulated STAT3 brain tumor suppressor pathway. Genes Dev 22(4):449–462. https://doi.org/10.1101/gad.1606508

44. Musteanu M, Blaas L, Mair M, Schlederer M, Bilban M, Tauber S, Esterbauer H, Mueller M, Casanova E, Kenner L, Poli V, Eferl R (2010) Stat3 is a negative regulator of intestinal tumor progression in Apc(Min) mice. Gastroenterology 138 (3):1003-1011 e1001-1005. https://doi.org/10.1053/j.gastro.2009.11.049

45. Schneller D, Machat G, Sousek A, Proell V, van Zijl F, Zulehner G, Huber H, Mair M, Muellner MK, Nijman SM, Eferl R, Moriggl R, Mikulits W (2011) p19(ARF) /p14(ARF) controls oncogenic functions of signal transducer and activator of transcription 3 in hepatocellular carcinoma. Hepatology 54(1):164–172. https://doi.org/10.1002/hep.24329

46. Wang H, Lafdil F, Wang L, Park O, Yin S, Niu J, Miller AM, Sun Z, Gao B (2011) Hepatoprotective versus oncogenic functions of STAT3 in liver tumorigenesis. Am J Pathol 179(2):714–724. https://doi.org/10.1016/j.ajpath.2011.05.005

47. Zhang HF, Lai R (2014) STAT3 in Cancer-friend or foe? Cancers (Basel) 6(3):1408–1440. https://doi.org/10.3390/cancers6031408

48. Yun UJ, Park SE, Jo YS, Kim J, Shin DY (2012) DNA damage induces the IL-6/STAT3 signaling pathway, which has anti-senescence and growth-promoting functions in human tumors. Cancer Lett 323(2):155–160. https://doi.org/10.1016/j.canlet.2012.04.003

49. Gottifredi V, McKinney K, Poyurovsky MV, Prives C (2004) Decreased p21 levels are required for efficient restart of DNA synthesis after S phase block. J Biol Chem 279(7):5802–5810. https://doi.org/10.1074/jbc.M310373200

50. Karimian A, Ahmadi Y, Yousefi B (2016) Multiple functions of p21 in cell cycle, apoptosis and transcriptional regulation after DNA damage. DNA Repair (Amst) 42:63–71. https://doi.org/10.1016/j.dnarep.2016.04.008

51. Deng T, Yan G, Song X, Xie L, Zhou Y, Li J, Hu X, Li Z, Hu J, Zhang Y, Zhang H, Sun Y, Feng P, Wei D, Hu B, Liu J, Tan W, Ye M (2018) Deubiquitylation and stabilization of p21 by USP11 is critical for cell-cycle progression and DNA damage responses. Proc Natl Acad Sci U S A 115(18):4678–4683. https://doi.org/10.1073/pnas.1714938115

52. Child ES, Mann DJ (2006) The intricacies of p21 phosphorylation: protein/protein interactions, subcellular localization and stability. Cell Cycle 5(12):1313–1319. https://doi.org/10.4161/cc.5.12.2863

53. Gartel AL, Tyner AL (2002) The role of the cyclin-dependent kinase inhibitor p21 in apoptosis 1 supported in part by NIH grant R01 DK56283 (to ALT) for the p21 research and campus research board and Illinois Department of Public Health penny Severns breast and cervical Cancer grants (to ALG). 1. Mol Cancer Ther 1(8):639–649

54. Fan Y, Borowsky AD, Weiss RH (2003) An antisense Oligodeoxynucleotide to p21Wafl/Cip1 causes apoptosis in human breast Cancer Cells1. Mol Cancer Ther 2(8):773–782

55. Stewart ZA, Mays D, Pietenpol JA (1999) Defective G1-S cell cycle checkpoint function sensitizes cells to microtubule inhibitor-induced apoptosis. Cancer Res 59(15):3831–3837

56. Waldman T, Lengauer C, Kinzler KW, Vogelstein B (1996) Uncoupling of S phase and mitosis induced by anticancer agents in cells lacking p21. Nature 381(6584):713–716

57. Weiss RH (2003) p21Wafl/Cip1 as a therapeutic target in breast and other cancers. Cancer Cell 4(6):425–429

58. Gartel AL, Tyner AL (2002) The role of the cyclin-dependent kinase inhibitor p21 in apoptosis. Mol Cancer Ther 1(8):639–649

59. Lin L, Hutzen B, Zuo M, Ball S, Deangelis S, Foust E, Pandit B, Ihnat MA, Shenoy SS, Kulp S, Li PK, Li C, Fuchs J, Lin J (2010) Novel STAT3 phosphorylation inhibitors exhibit potent growth-suppressive activity in pancreatic and breast cancer cells. Cancer Res 70(6):2445–2454. https://doi.org/10.1158/0008-5472.CAN-09-2468

60. Sonnenblick A, Brohée S, Fumagalli D, Vincent D, Venet D, Ignatiadis M, Salgado R, Van den Eynden G, Rothé F, Desmedt C (2015) Constitutive phosphorylated STAT3-associated gene signature is predictive for trastuzumab resistance in primary HER2-positive breast cancer. BMC Med 13(1):177

61. Timofeeva OA, Tarasova NI, Zhang X, Chasovskikh S, Cheema AK, Wang H, Brown ML, Dritschilo A (2013) STAT3 suppresses transcription of proapoptotic genes in cancer cells with the involvement of its N-terminal domain. Proc Natl Acad Sci 110(4):1267–1272